

# 1 **Single-molecule analysis of G protein-coupled receptor**

## 2 **stoichiometry: approaches and limitations**

3  
4 James H. Felce<sup>1\*</sup>, Simon J. Davis<sup>2</sup>, David Klenerman<sup>3</sup>

5  
6 <sup>1</sup> Kennedy Institute of Rheumatology, University of Oxford, Oxford OX3 7FY,  
7 United Kingdom.

8 <sup>2</sup> Radcliffe Department of Medicine and Medical Research Council Human  
9 Immunology Unit, Weatherall Institute of Molecular Medicine, University of Oxford,  
10 Oxford OX3 9DS, United Kingdom.

11 <sup>3</sup> Department of Chemistry, University of Cambridge, Cambridge CB2 1EW, United  
12 Kingdom.

13 \*Correspondence: james.felce@kennedy.ox.ac.uk

## 14 **Keywords**

15 Single-molecule imaging; GPCRs; BRET

## 16 **Abstract**

17 How G protein-coupled receptors (GPCRs) are organized at the cell surface remains  
18 highly contentious. Single-molecule (SM) imaging is starting to inform this debate as  
19 receptor behavior can now be visualized directly, without the need for interpreting  
20 ensemble data. The limited number of SM studies of GPCRs undertaken to date have  
21 strongly suggested that dimerization is at most transient, and that most receptors are  
22 monomeric at any given time. However, even SM data has its caveats and needs to be  
23 interpreted carefully. Here we discuss the types of SM imaging strategies used to  
24 examine GPCR stoichiometry and consider some of these caveats. We also emphasize  
25 that attempts to resolve the debate ought to rely on orthogonal approaches to  
26 measuring receptor stoichiometry.

## Introduction

### *Single molecule microscopy and G protein-coupled receptors*

One of the most powerful approaches for studying protein behavior *in situ* is single-molecule (SM) microscopy, which allows the tracking of individual proteins at the cell surface or in model membranes in one or more colors. Typically performed using total internal reflection fluorescence microscopy (TIRFM) to selectively illuminate only the basal 100-200 nm of a sample, SM imaging can yield a wealth of data relevant to the dynamics, distribution, and interactions of cell-surface proteins. In recent years, improvements in labeling strategies, fluorophores, and microscope sensitivity have extended the reach of SM imaging at a remarkable pace.

G protein-coupled receptors (GPCRs) represent the largest and pharmacologically most important family of cell surface receptors encoded by the human genome. Despite being the focus of intense study for over 20 years, perhaps the most contentious aspect of GPCR biology concerns their stoichiometry – *i.e.* whether they exist as monomers, dimers, or higher-order oligomers. Initially, *Rhodopsin*-family (class A) GPCRs were believed generally to be monomeric; however the present view is now shifted towards a model of dimeric and oligomeric complexes with distinct signaling behavior *in vivo* [1, 2]. This is still vigorously debated, however, mostly because a variety of techniques applied to many GPCRs have yielded often contradictory conclusions [arguments for and against oligomerization are summarized in the two articles: 3, 4].

Thus far, relatively few SM studies of GPCR stoichiometry have been undertaken, but these have profoundly influenced the debate, contributing to a shift away from constitutive dimerization toward one based on transient dimerization [5]. The status these studies have achieved is perhaps due to their being the first to offer stoichiometric information without the need to interpret bulk data, and the first to allow stoichiometry to be ‘seen’ directly. Here, we provide an overview of the SM-imaging approaches used to examine GPCR stoichiometry, including their important limitations, and reflect on their use to date.

### The diffraction limit

The principle constraint on conventional SM imaging is that resolution is set by the Abbe diffraction limit. Fluorophores separated by a distance smaller than this limit cannot be resolved, and so appear as a single object. Typically, this limit is 200-350 nm, *i.e.* 1-2 orders of magnitude greater than the diameter of most membrane proteins, and >20 times greater than the effective resolution of resonance energy transfer (RET) approaches (5-10 nm; discussed below). This is the most important confounding factor in the interpretation of SM-based stoichiometric studies, as it is impossible to distinguish genuine physical interactions from indirect co-localization within the resolvable distance. Super-resolution imaging-based SM approaches may eventually overcome this issue but have as yet had only a modest impact.

### *Measuring stoichiometry despite the diffraction limit*

Three methods are usually employed to determine the number of GPCRs within a fluorescent ‘spot’: spot-intensity analysis, photobleaching step counting, and two-color coincidence detection (TCCD; Figure 1). Spot-intensity analysis measures the absolute intensity of each spot and compares it to that for a single fluorophore. This approach is often combined with photobleaching-step counting, wherein the number of fluorophores in a spot is determined from the number of discrete intensities observed in the course of complete photobleaching. In TCCD experiments, receptors are labeled in two colors and the degree of co-localization between spots of opposite colors is measured [6]. Spots can also be tracked over time to allow their coincident movement to be observed.

These three approaches are presently the most effective means of determining stoichiometry in diffraction-limited SM imaging-based experiments, and yet none are without confounding issues of interpretation. In the first instance, more efficient detection of brighter spots could conceivably introduce bias. For example, this might involve the inappropriate use of thresholding below which weaker signals are discounted, or through subtler effects arising from the brightness and stability of the fluorophore used (see ‘Labeling considerations’). In intensity or photobleaching analyses this can skew the experiment toward detecting oligomers, since monomers will more likely go undetected. In TCCD, on the other hand, fewer dimers will be detected, as species containing two receptors of the same color will be preferentially detected, and counted as monomers. Similarly, all three analyses are sensitive to labeling efficiency, which must be taken into consideration. Most importantly, these

approaches only determine the number of receptors within a diffraction-limited area, not whether co-localization is direct (*i.e.* involving physical contact) or indirect (*i.e.* as a result of either chance proximity effects or ‘third-party’ associations); stoichiometry is therefore not reported directly.

#### *Dealing with indirect co-localization*

Researchers generally use two approaches to allow for indirect co-localization: simulations from first principles, and references to known controls. Monte Carlo simulations are used to determine the probable fraction of receptors co-localized by chance at the observed receptor densities. If particles are tracked over time, the likelihood of coincident movement due to chance can also be calculated by reference to the observed diffusional behavior. These models assume free diffusion and homogenous distribution of the receptors, with no anomalous behavior or interactions with ‘third-party’ proteins. They therefore tend to report expected background indirect co-localization levels that are very low [*e.g.* 7, 8].

However, it is now accepted that membrane proteins do not always exhibit free diffusion and can be highly constrained due to interactions with actin and/or other membrane/cytoskeletal elements [9-11]. In many cases, membrane proteins are heterogeneously distributed due to compartmentalization effects, ranging from small-scale ‘clustering’ to the large-scale effects of cell polarization. GPCR distributions are still poorly understood with regard to such effects, but there are reports of highly confined diffusion [12, 13], topologically-defined distribution [14, 15], and/or actin-dependent clustering [16]. The functional implications of these types of organization are still unclear. Differences in  $\beta$ -adrenergic receptor ( $\beta$ AR) organization in cardiac myocytes may explain subtype-specific variation in signaling behavior [17, 18], and alleviation of receptor segregation from signaling partners has been reported to increase basal signaling activity [19]. Irrespective of its functional importance or otherwise, the effects of nano- and micro-scale GPCR organization indicates that free-diffusion based modeling is likely incomplete, leading to substantial under-estimates of indirect co-localization or coincident movement and non-interacting receptors being incorrectly identified as oligomers.

The use of stoichiometric controls establishes the dynamic range of an experiment, allowing receptor stoichiometry to be assigned more rigorously. An

advantage of this approach over simulations is that it accommodates inefficiencies in labeling, or biases in spot detection, if the same labeling and detection strategies are used for controls and samples. Nonetheless, controls must be selected carefully to maximize similarities with sample receptors, since significant differences in either distribution or dynamics could alter their apparent stoichiometry relative to receptors of interest, rendering them unsuitable as controls. Unfortunately, this is not generally feasible in the case of *Rhodopsin*-family GPCRs, for which there are no agreed stoichiometric ‘exemplars’, and so researchers are limited to unrelated controls. The *Glutamate*-family GPCR  $\gamma$ -aminobutyric acid b receptor 2 (GABAbR2) is a well-established dimer [20, 21] used in a number of SM experiments [22, 23]. Monomer controls, however, have to be drawn from other protein families, typically type I transmembrane proteins [22, 23]. Whilst not ideal, these are nonetheless more appropriate controls than lipids [8], which exhibit vastly different diffusional properties versus transmembrane proteins. Finally, fixation removes the variable of differing dynamics between controls and samples [discussed at length in 22] leaving only nanoscale organization as a variable, which cannot be controlled for. Moreover, fixation precludes the study of dynamic processes, *e.g.* transient association.

In short, there is no perfect way to estimate the indirect co-localization rate in SM studies. Comparison to multiple well-characterized controls, on fixed cells, seems at the moment to be the best available option.

### **Labeling considerations**

The second major factor affecting the interpretation of SM studies is labeling strategy. GPCR labeling strategies have recently been exhaustively reviewed by Tian *et al.* [24]; however only a subset of these is suitable for stoichiometric analyses. The key issues for this are labeling efficiency, fluorophore brightness and stability, and tagged receptor activity. These matters are relevant to all SM experiments, but are particularly important in studies of stoichiometry since the outcome will be highly dependent on the fraction of detected receptors. Low labeling efficiency or photobleaching caused by poor fluorophore stability will lead to a substantial fraction of undetectable receptors, risking bias toward lower stoichiometry. Conversely, low fluorophore brightness can lead to overestimates of oligomer frequency since singly-tagged monomers will be more likely to go undetected.

### *Ligand-based strategies*

Near-perfect tagging of all cell-surface receptors on a given cell can be achieved with high-affinity, fluorophore-conjugated ligands, especially since a large number of bright, photostable fluorophores can be used. This approach has the major advantage of allowing investigation of endogenous receptors in native tissues, although target specificity needs to be confirmed to avoid the misidentification of off-target receptors. Moreover, fluorescent ligands are inherently intrusive, preclude the examination of GPCRs in the unliganded state, and are likely, unavoidably, to alter the behavior of target receptors. For example, the use of fluorescent agonists will lead to activation-driven internalization and/or clustering, shifting the apparent stoichiometry toward oligomers. This has been overcome in the past using internalization-deficient mutants [8] or by reconstituting receptors in high density lipoprotein particles [25], sacrificing a degree of physiological relevance. Nonetheless, even under these approaches the possibility exists that negative cooperativity (such that binding of one ligand to a dimer inhibits binding of a second [26]) may reduce apparent stoichiometry. Fluorescent antagonists have been used in studies of the M1 muscarinic receptor and dopamine D2 like receptor (D2L) expressed in Chinese Hamster Ovary (CHO) cells [7, 27], and the M2 receptor in primary mouse cardiomyocytes and cardiac tissue slices [28]. Antagonists, as opposed to inverse agonists, should not alter basal receptor activity and therefore, in principle, offer the best GPCR ligand-based labeling strategy. However, antagonists could in principle still interfere with receptor organization, and the ligand-based approach also precludes the use of stoichiometric controls as only the receptor of interest can be studied.

### *Genetically encoded fusion proteins*

The obvious alternative to ligand-based labeling strategies is to use genetically-encoded fusion proteins. This is generally less perturbative than using fluorescent ligands, but it requires expression in non-native cells to avoid the complication of interactions with unlabeled native receptors. Most often, human GPCRs have been transfected into CHO cells [e.g. 7, 22, 23, 29], thereby avoiding this problem, albeit at the cost of removing the receptors from their native context. It is unclear to what extent GPCR stoichiometry is cell-dependent, but it could in principle be influenced by cellular context, e.g. due to differences in membrane lipid environment [30] or

196 altered interactions with third-party proteins. An additional consideration is receptor  
197 density. SM imaging requires low densities allowing resolution of individual  
198 fluorophores and the minimization of indirect co-localization effects. However,  
199 transient dimerization could be highly dependent on receptor concentration, such that  
200 unphysiologically low densities might shift equilibria towards monomers. Examining  
201 a range of densities is the ideal approach but this might not always be feasible.

202         Several tagging strategies are suitable for SM imaging. Fluorescent proteins  
203 have the advantage of high labeling efficiency although they are typically less bright  
204 and/or photostable than inorganic dyes. Moreover, labeling is not necessarily  
205 complete since many fluorescent proteins exhibit imperfect folding and/or maturation  
206 [31, 32]. Receptors that are unlabeled due to misfolding of the attached fluorescent  
207 protein or photobleaching may reduce the apparent stoichiometry, whereas the  
208 relatively low brightness of some fluorescent proteins favors the detection of spots  
209 containing multiple receptors. It is therefore essential that analogously labeled  
210 stoichiometric controls are used to determine the dynamic range of the experiment.

211         The option of using brighter fluorophores is provided in the form of versatile  
212 enzyme-based fusion tags *e.g.* SNAP-tag [33], CLIP-tag [34], and HaloTag [35], each  
213 of which allows irreversible labeling with a series of inorganic dyes. Although bright  
214 and stable, labeling is relatively inefficient, meaning that stoichiometry can only be  
215 determined with reference to controls of known stoichiometry. Labeling efficiency  
216 varies substantially between C-terminal [ $<60\%$ ; 22] and N-terminal tags [ $<100\%$ ; 23]  
217 due to the relative availability of ligand inside and outside the cell. The improved  
218 labeling efficiency of extracellular tagging can come at the considerable cost of  
219 folding efficiency, however, because the N-terminal domain and associated  
220 transmembrane helix 1 are among the most folding-sensitive regions of GPCRs [36]  
221 and membrane transfer of the heterologous, fluorescent protein during translation can  
222 interfere with receptor folding [37]. In our experience, N-terminally tagged GPCRs  
223 frequently express and, by implication, fold less well than C-terminally tagged  
224 equivalents (unpublished data). This is likely to seriously hamper interpretations of  
225 stoichiometry because partial folding can induce aggregation and the false  
226 identification of oligomers. An alternative N-terminal labeling approach is to fuse  
227 receptors to small epitope tags, allowing *post hoc* targeting with fluorophore-  
228 conjugated monovalent antibody fragments [38].

229

## SM studies of GPCR stoichiometry

### *Initial studies of muscarinic receptors*

The first *in situ* SM analysis of GPCR stoichiometry was published by Hern *et al.* in 2010 [7] (a full list of SM imaging studies of GPCR stoichiometry is presented in Table 1). Their analysis of Cy3B antagonist-bound M1 revealed that >80% of spots had intensities consistent with single fluorophores, which exhibited single-step photobleaching. The remainder comprised spots likely to contain two antagonists (~8%), and others exhibiting apparent transitions between monomer and dimer states. TCCD-based analysis of mobile receptors labeled in two colors showed that ~80% exhibited independent movement, with the others diffusing coincidentally. The authors concluded that M1 receptors are predominantly monomeric, with ~30% of receptors forming short-lived dimers at any one time.

These observations were very important because they broke the hegemony in favor of constitutive M1 dimerization based previously on RET and co-immunoprecipitation experiments [e.g. 39]. The labeling approach meant that it was highly unlikely that the monomer population was overestimated as the fraction of unlabeled receptors was negligible. However, comparative stoichiometric controls were not possible, and so the extent if any of indirect co-localization had to be estimated using simulations. The probability of chance coincidence thus calculated was <1%, suggesting that the observed dimer fraction was largely genuine. Hern and colleagues justified their assumption of free diffusion by observing that the mean square displacement of receptors was linearly proportional to time, consistent with a random walk. However, as discussed above, it is unclear how reliable this assumption is. Slower diffusion of M1 upon dimerization was observed, as required by the Saffman-Delbrück model [40], consistent with genuine association. However, reduced diffusion might also have been caused indirectly by association with *e.g.* cytoskeletal proteins or membrane domains.

The same team subsequently performed the first SM investigation of GPCRs in native cells by probing M2 muscarinic receptors in mouse cardiomyocytes [28]. Photobleaching analysis revealed similar behavior to M1 in CHO cells: ~74% monomers in perinatal cardiomyocytes and ~57% in newborn myocytes. The remainder exhibited two-step photobleaching, whereas multi-step bleaching was not observed. This also confirmed that GPCRs do not constitutively dimerize *in situ*, in



contrast to conclusions based on a photobleaching-step analysis of isolated, immobilized M2 receptors suggesting tetrameric organization [41]. Nonetheless, the problem of how to interpret the apparent dimers remained. Indeed, the authors noted that the fraction of dimeric tracks increased with receptor density. This could arise either from a dynamic monomer-dimer equilibrium driven by a first-order binding process, or from increasing indirect coincidence at higher densities, or both. Intriguingly, the diffusion of M2 in isolated primary cardiomyocytes was ~4-fold slower than in fresh cardiac tissue slices, highlighting the need for studying receptors in their native settings.

#### *Subsequent SM studies reporting mostly monomers*

The original investigation by Hern *et al.* was followed shortly after by a similar analysis of an internalization-deficient *N*-formyl peptide receptor (FPR) expressed in CHO cells, labeled using a fluorescent agonist peptide [8]. Once again, ~60% of detected objects had intensities characteristic of monomers, consistent with previous observations [42]. The remaining ~40% of receptors behaved as dimers with average lifetimes far shorter than that of M1 [7]. Like Hern *et al.*, simulations of free diffusion were used to determine the chance coincidence rate. The authors did use monomeric controls, but one of these was an unsaturated phospholipid unlikely to exhibit similar distribution and diffusional properties to FPR, and the other was labeled with an alternative fluorophore, precluding direct intensity comparisons.

Comparable fractions of monomeric receptors were subsequently reported by Tabor *et al.* for D2L labeled with an N-terminal SNAP-tag and fluorescent ligands, expressed in CHO cells [27]. Spot-intensity analysis revealed ~70% monomers and ~30% apparent dimers, depending slightly on receptor density. A monomer control (the type I membrane protein, CD86) reported only 5% dimers. Similarly, ~80% and ~90% of the related D2S and D3 receptors behaved as monomers, respectively. Spot-intensity analysis of GFP-tagged apelin receptors in CHO cells also implied that monomers were the largest single population present, comprising 40% of receptors, with 36% forming apparent dimers, and 24% oligomers [29]. However, the contribution of indirect co-localization was not addressed.

The extent to which indirect co-localization might have affected the interpretation of each of these studies is difficult to estimate. A study using fixed cells and benchmarking with monomeric and dimeric controls examined C-terminally

Halo- and SNAP-tagged  $\beta_2$ AR and mCannR2 expressed in HEK 293T and CHO cells [22]. TCCD analysis showed that neither GPCR exhibited coincidence above that of a monomeric control protein, whereas the two dimer controls exhibited coincidence levels 2-3 fold higher. Significantly, and similar to the observations of Tabor *et al.* [27], the monomer control (CD86) exhibited ~8-10% coincidence, showing that even known monomers exhibit a degree of indirect co-localization. This was the first *in situ* SM analysis to report the absence of detectable dimerization for any *Rhodopsin*-family GPCR. This analysis has more recently been extended to  $\beta_1$ AR and the lysophosphatidic acid receptor 1 (LPA1), which behaved as monomers; and the closely related  $\alpha_{2C}$ -adrenergic receptor ( $\alpha_{2C}$ AR) and sphingosine-1-phosphate receptor 3 (S1P3), which behaved as dimers [43]. It is also noteworthy that a purified and functionally reconstituted GPCR, the  $\mu$ -opioid receptor ( $\mu$ -OR) also failed to self-organize, indicating that at a protein-intrinsic level, this receptor is monomeric [25].

#### *A SM study reporting predominantly oligomers*

Whilst there is some uncertainty about the authenticity of the GPCR oligomers observed in SM studies done to date there is, however, the consistent finding that dimerization is not constitutive. Indeed, only one SM study reports that a receptor forms mostly dimeric/oligomeric complexes. N-terminally SNAP-tagged  $\beta_1$ AR and  $\beta_2$ AR expressed in CHO cells were subjected to spot-intensity analysis by Calebiro *et al.*, and 30-85% of  $\beta_1$ AR, and 60-100% of  $\beta_2$ AR receptors exhibited intensities greater than that expected for monomers. At high densities both receptors formed apparent trimers, tetramers, and higher-order oligomers. Indirect co-localization was addressed using free diffusion-based simulations.

As the only GPCRs examined in multiple separate SM analyses, it is striking that the studies of  $\beta_1$ AR and  $\beta_2$ AR by Calebiro *et al.*, and by Latty *et al.* and Felce *et al.*, have produced such different outcomes. The reasons for the discrepancies are difficult to ascertain since there were many differences between the approaches taken, including the measurement strategy (intensity analysis vs. TCCD), expression system (stable vs. transient), cell context (live vs. fixed), and labeling strategy (N-terminal vs. C-terminal). As discussed above, it is possible that N-terminal labeling of  $\beta$ ARs by Calebiro *et al.* resulted in partial aggregation of the receptors leading to increased detection of oligomers. The authors reported normal receptor responses to ligand, suggesting that at least some of the  $\beta$ ARs were active, but not necessarily all.

Alternatively, the use of intensity analysis rather than TCCD could explain the higher levels of apparent receptor oligomerization if detection bias for brighter spots was introduced into the analysis. The observation that 0% of a double-labeled dimer control used by Calebiro behaved as a monomer offers some support for this view, because a degree of monomeric behavior should have been observable due to imperfect labeling efficiency. The SNAP-tag used by Calebiro *et al.* is a derivative of the DNA repair protein O6-alkylguanine-DNA alkyltransferase [33], and undergoes low level conjugation to non-fluorescent benzylguanine moieties within the cell, precluding 100% fluorescence labeling. A final, formal possibility is that the labeling efficiencies, determined only for the controls in Latty *et al.* and Felce *et al.*, differ for the controls versus the GPCRs studied, although there are no reports of Halo- or SNAP-tag labeling being dependent on their fusion partners.

### **Super-resolution based studies**

Presently, SM super-resolution imaging comprises photoactivated localization microscopy (PALM) and stochastic optical reconstruction microscopy (STORM), which temporally separate emission from individual fluorophores to allow calculation of position with sub-diffraction precision. Applied to stoichiometric measurements, the effective resolution of PALM/STORM experiments (10-30 nm) offers greater discrimination between genuine interactions and indirect co-localization. On this scale the chance co-localization rate for randomly distributed GPCRs at typical densities (0.1-1 receptors/ $\mu\text{m}^2$ ) is effectively zero. Nonetheless, the method cannot yet distinguish between directly interacting receptors and those interacting locally with a common partner (*e.g.* actin). Super-resolution imaging is also vulnerable to reporting artifactual protein clustering due to imperfect fixation [44, 45], or repeated detection of a fluorophore due to stochastic blinking behavior [46].

The first PALM-based study of a GPCR measured the fraction of  $\beta_2\text{AR}$  molecules in >5 molecule clusters rather than base stoichiometry *per se*, reporting that clustering varied significantly between cell types [16]. Cryogenic localization microscopy has been used to examine relative spacing of receptors within dimers [27] but only recently has GPCR stoichiometry been directly examined using super-resolution SM imaging [38]. Jonas *et al.* examined the luteinizing hormone receptor (LHR) tagged N-terminally with epitope tags bound by antibodies conjugated to

photoactivatable dyes. Using PALM, they localized receptors with a precision of ~20 nm, representing an ~10-fold improvement over diffraction-limited SM approaches, and found that ~14% of LHR spots associated with another (consistent with dimerization) while ~27% associate with >1, including ~10% within clusters of >9 receptors. By analyzing the spot separation within trimeric and tetrameric clusters they proposed a model of protomer assembly producing a diverse range of receptor complexes. Importantly, however, ~60% of LHR is wholly monomeric, consistent with most SM studies. Whether the observed associations represent *bona fide* interactions is unclear. Although the levels of indirect co-localization for randomly distributed receptors at this resolution is extremely low, the authors acknowledge that observed oligomers may be the product of receptor clustering at some form of membrane or cytoskeletal structure. A monomeric control also exhibited a dimeric fraction of ~11%, marginally lower than LHR (~14%), suggesting that a fraction of the detected dimers were the product of indirect co-localizations. Low-level clustering detected as higher-order oligomerization might result from basal receptor activity [a common feature of GPCRs; 47]. The observation that a signaling-deficient mutant produced more monomeric behavior when in excess over a binding-deficient mutant is consistent with such an effect, as the reduced basal signaling would likely lead to relaxed clustering and fewer apparent oligomers.

### **The value of orthogonal approaches**

SM imaging has, of course, emerged alongside existing methods of stoichiometric analysis. In bimolecular fluorescence complementation (BiFC), which has been employed in parallel with conventional SM imaging in a number studies, two inactive fluorescent-protein fragments form a fluorescent complex when fused to interacting pairs of proteins. However, a significant problem with BiFC is that the formation of the fluorescent complex is essentially irreversible [48-50], and so capable of stabilizing non-physiological interactions of membrane proteins. Kasai *et al.* [8] and Cai *et al.* [29] have used BiFC to analyze the FPR and the apelin receptor, respectively. Since Kasai *et al.* found that fluorescent BiFC spots had average lifetimes of 301 ms (three-fold longer than observed in their SM tracking experiments) it seems that there could have been a degree of complex stabilization, confounding interpretation of the data.

Arguably, studies utilizing the RET-based assays Förster (FRET) and bioluminescence RET (BRET) have had the largest impact on the stoichiometry debate. Energy transfer efficiencies ( $\text{RET}_{\text{eff}}$ ) between donor and acceptor molecules is negligible above a separation distance of 5-10 nm, conferring upon RET assays an effective resolution far superior to that of SM imaging. RET-based assays are therefore highly complementary to the SM approach. However, the interpretation of RET assays of membrane proteins is also complicated by indirect interactions. Remarkably, expressed as ‘BRET pairs’, monomers exhibit  $\text{BRET}_{\text{eff}}$  equivalent to ~25% that of covalent dimers [51], and so the occurrence of RET alone cannot be used to infer oligomerization. Nonetheless, RET alone, both in transfected cell systems [*e.g.* 52, 53] and native tissues [*e.g.* 54] has, even in the recent past, been used as the sole basis for claiming oligomerization.

Most RET studies now attempt to distinguish specific and non-specific RET using several approaches. The most common is the BRET saturation assay, wherein donor concentration is kept constant and acceptor levels are systematically increased [55]. Despite widespread use, its reliance on distinguishing between a pseudolinear increase in  $\text{BRET}_{\text{eff}}$  for monomers and a hyperbolic one for dimers greatly complicates the interpretation of this type of data [56]. First, distinguishing between two systematically increasing signals can be difficult unless the data are of exceptional quality. Second, the assumption of pseudolinearity for monomeric proteins can be unsafe in certain circumstances at high receptor expression [57]. We have described elsewhere BRET assays that circumvent these issues by maintaining either a constant receptor density (the ‘type-1’ assay) or constant acceptor:donor ratio [the ‘type-2’ assay; 51, 56]. The principle of the type-1 assay is illustrated in Figure 2a, and its ability to distinguish between monomers and both transient and covalent dimers illustrated in Figure 2b. We have also developed an adapted competition assay [the ‘type-3’ assay; 57], which uses untagged ‘competitor’ proteins to disrupt genuine BRET-productive association whilst accounting for the effect of competitors on the expression of tagged proteins. In these types of assays, for well-behaving proteins *and with the use of suitable controls*, it is a straightforward matter to distinguish between monomers and dimers. BRET assays also offer the advantage, over SM methods, of being implementable in semi-high-throughput settings, allowing large scale comparative studies [43]. The debate over the correct implementation of BRET for stoichiometric analysis [58-60] has, we suspect, somewhat diminished enthusiasm for

this general approach. This would be unfortunate if true because, used in the right way, these assays are very powerful tools in their own right, and especially well-suited to validating conclusions derived from SM imaging.

### **Future perspectives**

The most pressing current need is for a broader range of receptors to be tested using SM imaging to build up a clearer model of GPCR organization and behavior, particularly through increasingly unambiguous super-resolution approaches. Alongside super-resolution imaging technology *per se*, significant advances in receptor labeling may increase the power of the SM approach. To improve spatial resolution, DNA-PAINT (point accumulation for imaging in nanoscale topography) uses transient binding of short fluorescent oligonucleotides to DNA-tagged proteins to greatly increase overall photon count, and therefore localization precision [61]. The ~5 nm achievable resolution of DNA-PAINT could potentially report GPCR stoichiometry on a single-receptor scale, overcoming many of the interpretive issues of lower-resolution approaches discussed here. Similarly, multicolor quantum dot ligands for the HaloTag labeling system offer far greater temporal resolution than current approaches due to their extreme photostability [62], and will likely provide greater insight into possible transient dimerization, if this occurs. This, and other genetic tagging strategies, will be facilitated by Cas9-targeted homology directed repair [63], allowing their use in native cells, away from potentially inappropriate cellular contexts. This will also ensure native receptor expression levels, which will be advantageous because the physiological concentrations of most GPCRs are not well understood, and most studies have not performed density-dependent measurements that would allow extrapolation to a range of densities. In general, a move towards examining receptors in primary cells is important given the possibility that the distribution of some GPCRs might be controlled in native tissues. Indeed, it will be the combination of stoichiometry and microscale organization that will be vital to fully understanding GPCR behavior, since organization may be equally or more important than stoichiometry for regulating some receptors [e.g. 15, 64].

### **Concluding Remarks**

The debate about GPCR stoichiometry has been ongoing since the first suggestions of generalized dimerization fifteen years ago [65, 66]. SM imaging entered the discourse relatively recently, at a time when many, often contradictory biochemical and biophysical studies had failed to produce a clear consensus (see ‘Outstanding Questions’). The insights generated by the small number of published GPCR SM studies have already been substantial; but even the critical interpretation of these data is not trivial. It seems likely, therefore, that a satisfactory answer to the GPCR stoichiometry question will depend heavily on SM imaging, supported by other technologies. The more different ways we can make our observations, the more confidence we can have in the answers we obtain. The truth will be marked by a convergence of observations.

#### **Conflict of Interest**

The authors declare that they have no conflicts of interest.

1. Pflieger, K.D.G. and Eidne, K.A. (2005) Monitoring the formation of dynamic G-protein-coupled receptor-protein complexes in living cells. *Biochemical Journal* 385, 625-637.
2. Petrin, D. and Hebert, T.E. (2012) The functional size of GPCRs - monomers, dimers or tetramers? *Sub-cellular biochemistry* 63, 67-81.
3. Bouvier, M. and Hebert, T.E. (2014) CrossTalk proposal: Weighing the evidence for Class A GPCR dimers, the evidence favours dimers. *Journal of Physiology-London* 592 (12), 2439-2441.
4. Lambert, N.A. and Javitch, J.A. (2014) CrossTalk opposing view: Weighing the evidence for classA GPCR dimers, the jury is still out. *Journal of Physiology-London* 592 (12), 2443-2445.
5. Lambert, N.A. (2010) GPCR Dimers Fall Apart. *Science Signaling* 3 (115).
6. Dunne, P.D. et al. (2009) DySCo: Quantitating Associations of Membrane Proteins Using Two-Color Single-Molecule Tracking. *Biophysical Journal* 97 (4), L5-L7.
7. Hern, J.A. et al. (2010) Formation and dissociation of M-1 muscarinic receptor dimers seen by total internal reflection fluorescence imaging of single molecules. *Proceedings of the National Academy of Sciences of the United States of America* 107 (6), 2693-2698.
8. Kasai, R.S. et al. (2011) Full characterization of GPCR monomer-dimer dynamic equilibrium by single molecule imaging. *Journal of Cell Biology* 192 (3), 463-480.
9. Kusumi, A. et al. (2012) Membrane mechanisms for signal transduction: The coupling of the meso-scale raft domains to membrane-skeleton-induced compartments and dynamic protein complexes. *Seminars in Cell & Developmental Biology* 23 (2), 126-144.
10. Kusumi, A. et al. (2011) Hierarchical mesoscale domain organization of the plasma membrane. *Trends in Biochemical Sciences* 36 (11), 604-615.

- 512 11. Bernardino de la Serna, J. et al. (2016) There is no simple model of the  
513 plasma membrane organization. *Frontiers in Cell and Developmental Biology* 4  
514 (106).
- 515 12. Dumas, F. et al. (2003) Confined diffusion without fences of a G-protein-  
516 coupled receptor as revealed by single particle tracking. *Biophysical Journal* 84  
517 (1), 356-366.
- 518 13. Suzuki, K. et al. (2005) Rapid hop diffusion of a G-protein-coupled receptor in  
519 the plasma membrane as revealed by single-molecule techniques. *Biophysical*  
520 *Journal* 88 (5), 3659-3680.
- 521 14. Ianoul, A. et al. (2005) Imaging nanometer domains of beta-adrenergic  
522 receptor complexes on the surface of cardiac myocytes. *Nature Chemical Biology*  
523 1 (4), 196-202.
- 524 15. Nikolaev, V.O. et al. (2010) beta(2)-Adrenergic Receptor Redistribution in  
525 Heart Failure Changes cAMP Compartmentation. *Science* 327 (5973), 1653-1657.
- 526 16. Scarselli, M. et al. (2012) Cell Type-specific beta 2-Adrenergic Receptor  
527 Clusters Identified Using Photoactivated Localization Microscopy Are Not Lipid  
528 Raft Related, but Depend on Actin Cytoskeleton Integrity. *Journal of Biological*  
529 *Chemistry* 287 (20), 16768-16780.
- 530 17. Xiang, Y. and Kobilka, B.K. (2003) Myocyte adrenoceptor signaling pathways.  
531 *Science* 300 (5625), 1530-1532.
- 532 18. Xiang, Y. et al. (2002) Caveolar localization dictates physiologic signaling of  
533 beta(2)-adrenoceptors in neonatal cardiac myocytes. *Journal of Biological*  
534 *Chemistry* 277 (37), 34280-34286.
- 535 19. Pontier, S.M. et al. (2008) Cholesterol-dependent Separation of the beta(2)-  
536 Adrenergic Receptor from Its Partners Determines Signaling Efficacy: Insight  
537 into nanoscale organization of signal transduction. *Journal of Biological*  
538 *Chemistry* 283 (36), 24659-24672.
- 539 20. Jones, K.A. et al. (1998) GABA(B) receptors function as a heteromeric  
540 assembly of the subunits GABA(B)R1 and GABA(B)R2. *Nature* 396 (6712), 674-  
541 679.
- 542 21. Margeta-Mitrovic, M. et al. (2000) A trafficking checkpoint controls GABA(B)  
543 receptor heterodimerization. *Neuron* 27 (1), 97-106.
- 544 22. Latty, S.L. et al. (2015) Referenced Single-Molecule Measurements  
545 Differentiate between GPCR Oligomerization States. *Biophysical Journal* 109 (9),  
546 1798-1806.
- 547 23. Calebiro, D. et al. (2013) Single-molecule analysis of fluorescently labeled G-  
548 protein-coupled receptors reveals complexes with distinct dynamics and  
549 organization. *Proceedings of the National Academy of Sciences of the United*  
550 *States of America* 110 (2), 743-748.
- 551 24. Tian, H. et al. (2017) Labeling and Single-Molecule Methods To Monitor G  
552 Protein-Coupled Receptor Dynamics. *Chemical Reviews* 117 (1), 186-245.
- 553 25. Kuszak, A.J. et al. (2009) Purification and Functional Reconstitution of  
554 Monomeric mu-Opioid Receptors: Allosteric modulation of agonist binding by  
555 Gi2. *Journal of Biological Chemistry* 284 (39), 26732-26741.
- 556 26. Vischer, H.F. et al. (2011) G protein-coupled receptors: walking hand-in-  
557 hand, talking hand-in-hand? *British Journal of Pharmacology* 163 (2), 246-260.
- 558 27. Tabor, A. et al. (2016) Visualization and ligand-induced modulation of  
559 dopamine receptor dimerization at the single molecule level. *Scientific Reports* 6.



28. Nenasheva, T.A. et al. (2013) Abundance, distribution, mobility and oligomeric state of M-2 muscarinic acetylcholine receptors in live cardiac muscle. *Journal of Molecular and Cellular Cardiology* 57, 129-136.
29. Cai, X. et al. (2017) Apelin receptor homodimer-oligomers revealed by singlemolecule imaging and novel G protein-dependent signaling. *Scientific Reports* 7.
30. Bolivar, J.H. et al. (2016) Interaction of lipids with the neurotensin receptor 1. *Biochimica Et Biophysica Acta-Biomembranes* 1858 (6), 1278-1287.
31. Pedelacq, J.D. et al. (2006) Engineering and characterization of a superfolder green fluorescent protein. *Nature Biotechnology* 24 (1), 79-88.
32. Hebisch, E. et al. (2013) High Variation of Fluorescence Protein Maturation Times in Closely Related *Escherichia coli* Strains. *Plos One* 8 (10).
33. Keppler, A. et al. (2003) A general method for the covalent labeling of fusion proteins with small molecules in vivo. *Nature Biotechnology* 21 (1), 86-89.
34. Gautier, A. et al. (2008) An engineered protein tag for multiprotein labeling in living cells. *Chemistry & Biology* 15 (2), 128-136.
35. Los, G.V. et al. (2008) HatoTag: A novel protein labeling technology for cell imaging and protein analysis. *Acs Chemical Biology* 3 (6), 373-382.
36. Schlinkmann, K.M. et al. (2012) Critical features for biosynthesis, stability, and functionality of a G protein-coupled receptor uncovered by all-versus-all mutations. *Proceedings of the National Academy of Sciences of the United States of America* 109 (25), 9810-15.
37. Feilmeier, B.J. et al. (2000) Green fluorescent protein functions as a reporter for protein localization in *Escherichia coli*. *Journal of Bacteriology* 182 (14), 4068-4076.
38. Jonas, K.C. et al. (2015) Single Molecule Analysis of Functionally Asymmetric G Protein-coupled Receptor (GPCR) Oligomers Reveals Diverse Spatial and Structural Assemblies. *Journal of Biological Chemistry* 290 (7), 3875-3892.
39. Goin, J.C. and Nathanson, N.M. (2006) Quantitative analysis of muscarinic acetylcholine receptor homo- and heterodimerization in live cells - Regulation of receptor down-regulation by heterodimerization. *Journal of Biological Chemistry* 281 (9), 5416-5425.
40. Saffman, P.G. and Delbruck, M. (1975) Brownian motion in biological membranes. *Proceedings of the National Academy of Sciences of the United States of America* 72 (8), 3111-3113.
41. Shivnaraine, R.V. et al. (2016) Single-Molecule Analysis of the Supramolecular Organization of the M2 Muscarinic Receptor and the G alpha(i1) Protein. *Journal of the American Chemical Society* 138 (36), 11583-11598.
42. Gripentrog, J.M. et al. (2003) Experimental evidence for lack of homodimerization of the G protein-coupled human N-formyl peptide receptor. *Journal of Immunology* 171 (6), 3187-3193.
43. Felce, J.H. et al. (2017) Receptor quaternary organization explains G protein-coupled receptor family structure. *Cell Reports* 20 (11), 2654-2665.
44. Tanaka, K.A.K. et al. (2010) Membrane molecules mobile even after chemical fixation. *Nature Methods* 7 (11), 865-866.
45. Stanly, T.A. et al. (2016) Critical importance of appropriate fixation conditions for faithful imaging of receptor microclusters. *Biology Open* 5 (9), 1343-1350.

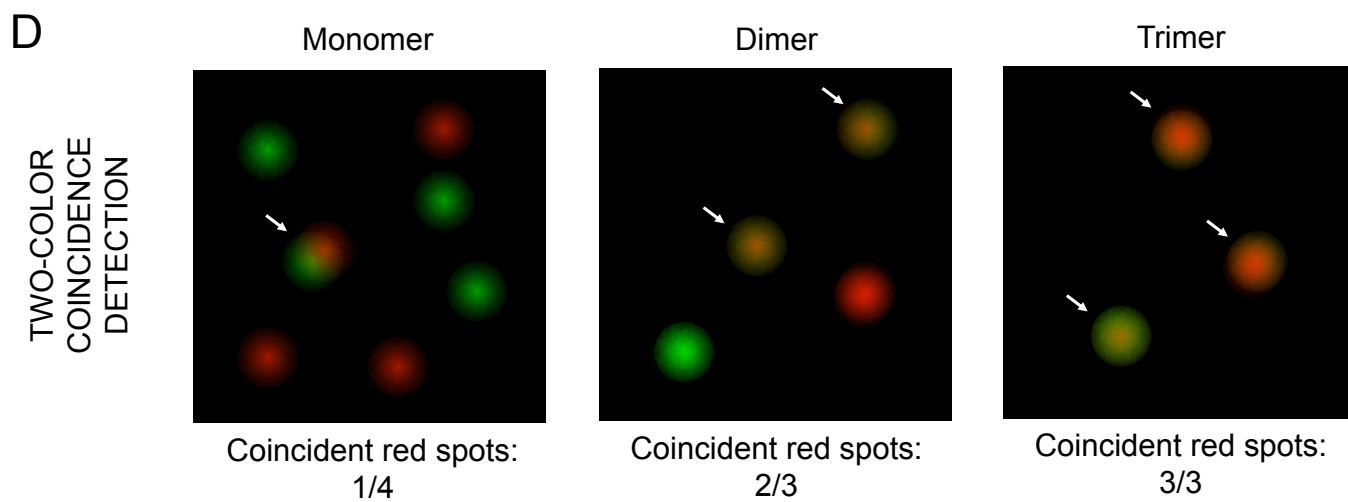
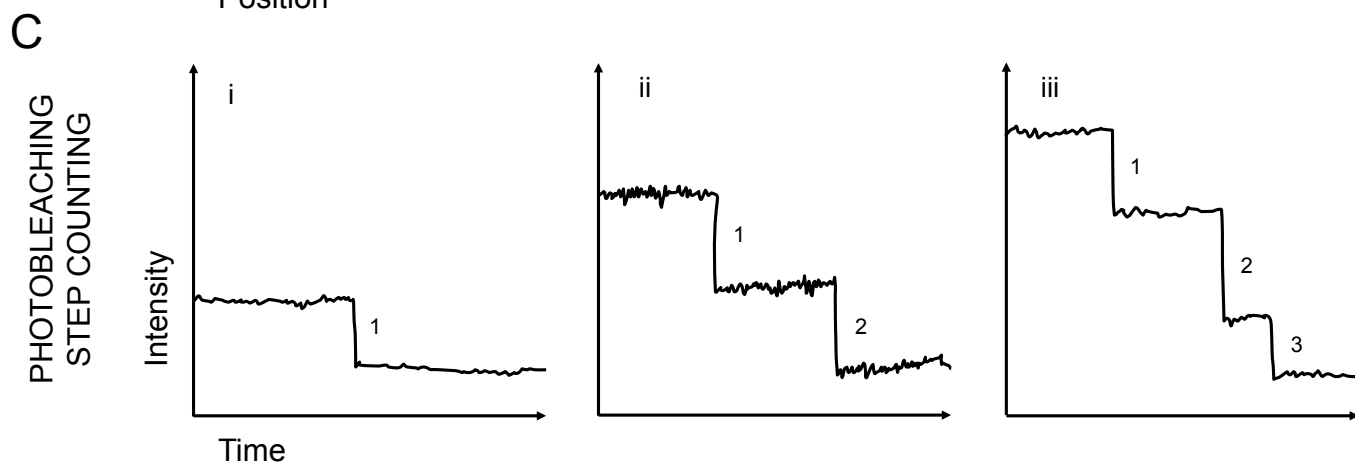
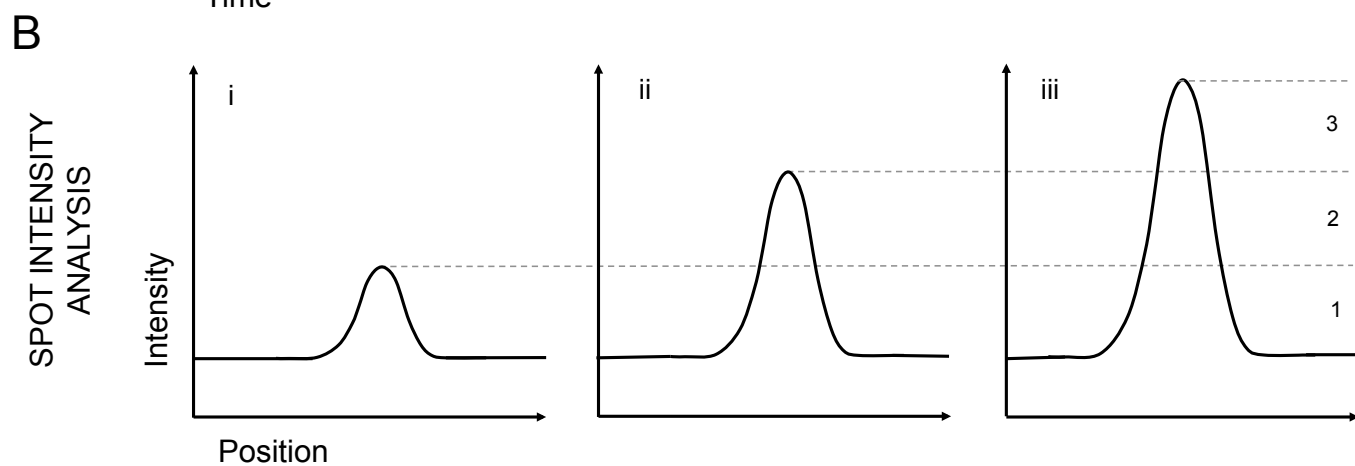
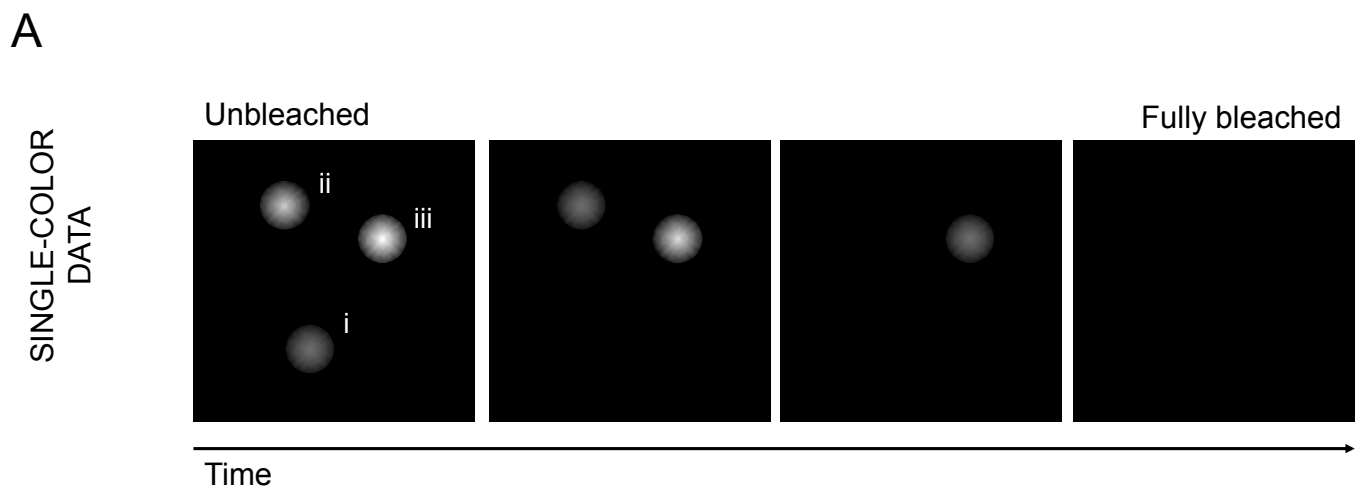
- 608 46. Baumgart, F. et al. (2016) Varying label density allows artifact-free analysis  
609 of membrane-protein nanoclusters. *Nature Methods* 13 (8), 661-+.
- 610 47. Kobilka, B.K. and Deupi, X. (2007) Conformational complexity of G-protein-  
611 coupled receptors. *Trends in Pharmacological Sciences* 28 (8), 397-406.
- 612 48. Hu, C.D. et al. (2002) Visualization of interactions among bZip and Rel family  
613 proteins in living cells using bimolecular fluorescence complementation.  
614 *Molecular Cell* 9 (4), 789-798.
- 615 49. Morell, M. et al. (2008) Monitoring the interference of protein-protein  
616 interactions in vivo by bimolecular fluorescence complementation: the DnaK  
617 case. *Proteomics* 8 (17), 3433-3442.
- 618 50. Kerppola, T.K. (2006) Design and implementation of bimolecular  
619 fluorescence complementation (BiFC) assays for the visualization of protein  
620 interactions in living cells. *Nature Protocols* 1 (3), 1278-1286.
- 621 51. James, J.R. et al. (2006) A rigorous experimental framework for detecting  
622 protein oligomerization using bioluminescence resonance energy transfer.  
623 *Nature Methods* 3 (12), 1001-1006.
- 624 52. Ramsay, D. et al. (2002) Homo- and hetero-oligomeric interactions between  
625 G-protein-coupled receptors in living cells monitored by two variants of  
626 bioluminescence resonance energy transfer (BRET): hetero-oligomers between  
627 receptor subtypes form more efficiently than between less closely related  
628 sequences. *Biochemical Journal* 365, 429-440.
- 629 53. Yoshioka, K. et al. (2002) Agonist-promoted heteromeric oligomerization  
630 between adenosine A(1) and P2Y(1) receptors in living cells. *Febs Letters* 523  
631 (1-3), 147-151.
- 632 54. Albizu, L. et al. (2010) Time-resolved FRET between GPCR ligands reveals  
633 oligomers in native tissues. *Nature Chemical Biology* 6 (8), 587-594.
- 634 55. Ayoub, M.A. and Pflieger, K.D.G. (2010) Recent advances in bioluminescence  
635 resonance energy transfer technologies to study GPCR heteromerization. *Current*  
636 *Opinion in Pharmacology* 10 (1), 44-52.
- 637 56. Felce, J.H. and Davis, S.J. (2012) Unraveling Receptor Stoichiometry Using  
638 BRET. *Frontiers in endocrinology* 3 (86).
- 639 57. Felce, J.H. et al. (2014) Type-3 BRET, an Improved Competition-Based  
640 Bioluminescence Resonance Energy Transfer Assay. *Biophysical Journal* 106  
641 (12), L41-L43.
- 642 58. Bouvier, M. et al. (2007) BRET analysis of GPCR oligomerization: newer does  
643 not mean better. *Nature Methods* 4 (1), 3-4.
- 644 59. Salahpour, A. and Masri, B. (2007) Experimental challenge to a 'rigorous'  
645 BRET analysis of GPCR oligomerization. *Nature Methods* 4 (8), 599-600.
- 646 60. James, J.R. and Davis, S.J. (2007) Experimental challenge to a 'rigorous' BRET  
647 analysis of GPCR oligomerization - James and Davis reply. *Nature Methods* 4 (8),  
648 601-601.
- 649 61. Schnitzbauer, J. et al. (2017) Super-resolution microscopy with DNA-PAINT.  
650 *Nature Protocols* 12 (6), 1198-1228.
- 651 62. Komatsuzaki, A. et al. (2015) Compact Halo-Ligand-Conjugated Quantum  
652 Dots for Multicolored Single-Molecule Imaging of Overcrowding GPCR Proteins  
653 on Cell Membranes. *Small* 11 (12), 1396-1401.
- 654 63. Ran, F.A. et al. (2013) Genome engineering using the CRISPR-Cas9 system.  
655 *Nature Protocols* 8 (11), 2281-2308.

- 656 64. Surdo, N.C. et al. (2017) FRET biosensor uncovers cAMP nano-domains at  
657 beta-adrenergic targets that dictate precise tuning of cardiac contractility.  
658 Nature Communications 8.
- 659 65. Angers, S. et al. (2002) Dimerization: An emerging concept for G protein-  
660 coupled receptor ontogeny and function. Annual Review of Pharmacology and  
661 Toxicology 42, 409-435.
- 662 66. George, S.R. et al. (2002) G-protein-coupled receptor oligomerization and its  
663 potential for drug discovery. Nature Reviews Drug Discovery 1 (10), 808-820.  
664  
665

## FIGURE LEGENDS

**Figure 1** – SM imaging-based approaches to determining protein stoichiometry. **(A)** In single-color experiments, spots are detected in one channel for one or more frames. The four panels depict the simulated step-wise photobleaching of a monomer (*i*), dimer (*ii*), and trimer (*iii*) over time, at a constant rate (loss of one fluorophore from each object per panel). **(B)** Intensity analysis gives the number of labeled proteins in a spot by comparing the starting (*i.e.* unbleached) fluorescence to that of a single fluorophore. Spots should exhibit discrete intensity levels corresponding to multiples of the single fluorophore intensity (*i.e.*  $i = 1$  fluorophore,  $ii = 2$ ,  $iii = 3$ ). Simulated data is shown. **(C)** Photobleaching-step counting requires spot tracking for multiple frames, during which photobleaching should occur in discrete steps corresponding to the bleaching of individual fluorophores in the spot (*i.e.*  $i = 1$  bleaching event,  $ii = 2$ ,  $iii = 3$ ). Simulated data is shown. **(D)** TCCD involves detecting spots in two colors and determining the fraction of spots in one color that are within a specified radius of spots in the other color. This yields a coincidence value that is then compared to those of known stoichiometric controls. The three panels depict simulated images of receptors labeled in two colors at a constant 4:4 red:green ratio. The fraction of red spots identified as coincident below each panel corresponds to the number of spots comprising at least one receptor in each color (white arrows) divided by the total number of spots comprising at least one red receptor.

**Figure 2** – Principles of the type-1 BRET assay. **(A)** In a type-1 BRET experiment, acceptor/donor ratio is increased but surface density is kept constant by exchanging donors for acceptors (as indicated within the red circles). For a monomer,  $BRET_{eff}$  is unchanged, whereas for a dimer  $BRET_{eff}$  increases as the fraction of productive dimers increases. Donor-tagged proteins are represented as blue circles with a BRET-permissive halo. Fluorescing and non-fluorescing acceptors are illustrated as green-filled or white-filled circles, respectively.  $BRET_{eff}$  (calculated under each panel) is determined as the fraction of donor molecules within the BRET-permissive radius of one or more acceptor molecules. **(B)** Characteristic type-1 BRET data for monomeric transmembrane proteins (CD86, CD2), and for transient (CD80), or covalent (CD28) transmembrane protein dimers. The relationship between  $BRET_{eff}$  and acceptor:donor ratio matches a hyperbolic fit (solid line) for dimers but is invariant above a acceptor:donor ratio of  $\sim 2$  (broken line) for monomers, consistent with the model shown in Figure 2A. Data reproduced with permission from James *et al.*, 2006 [51].



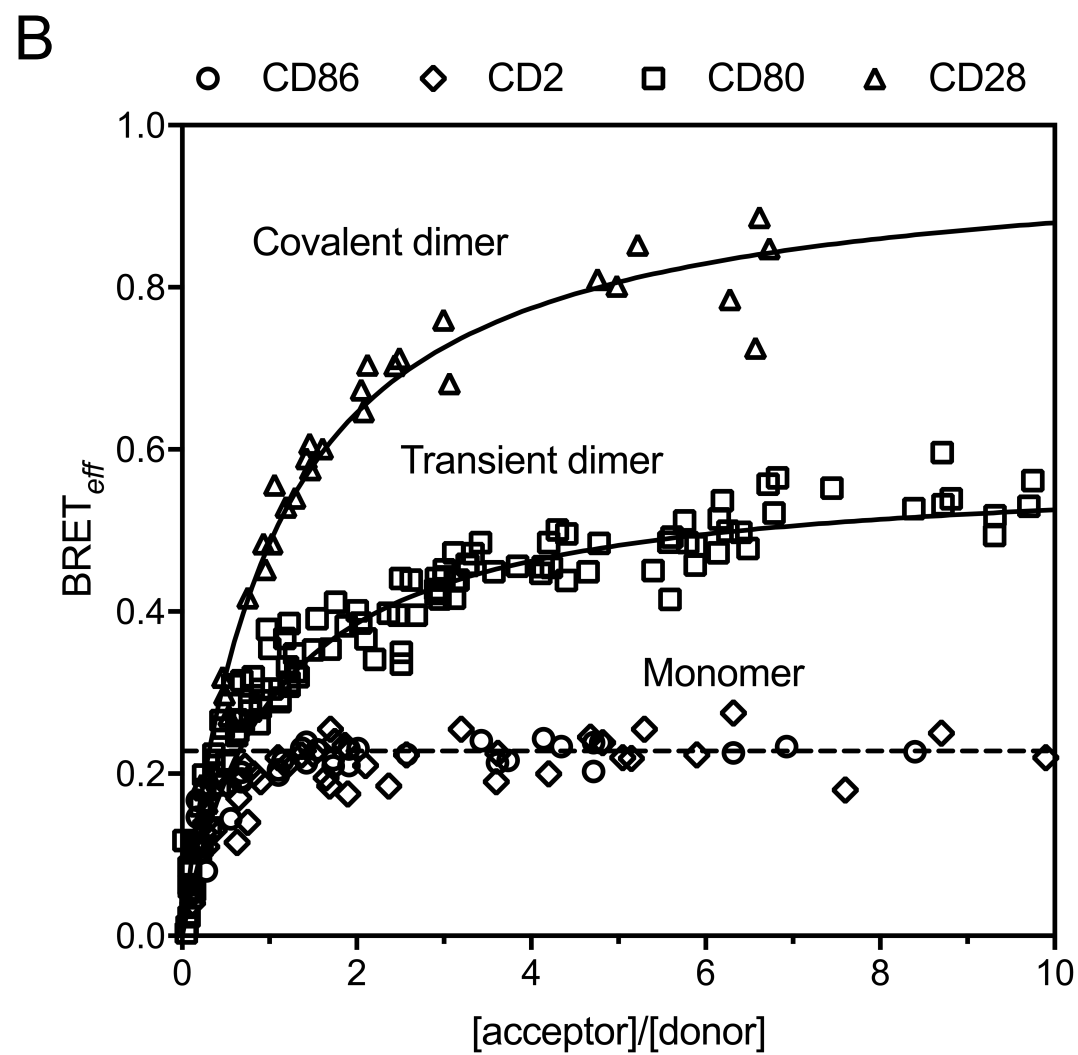
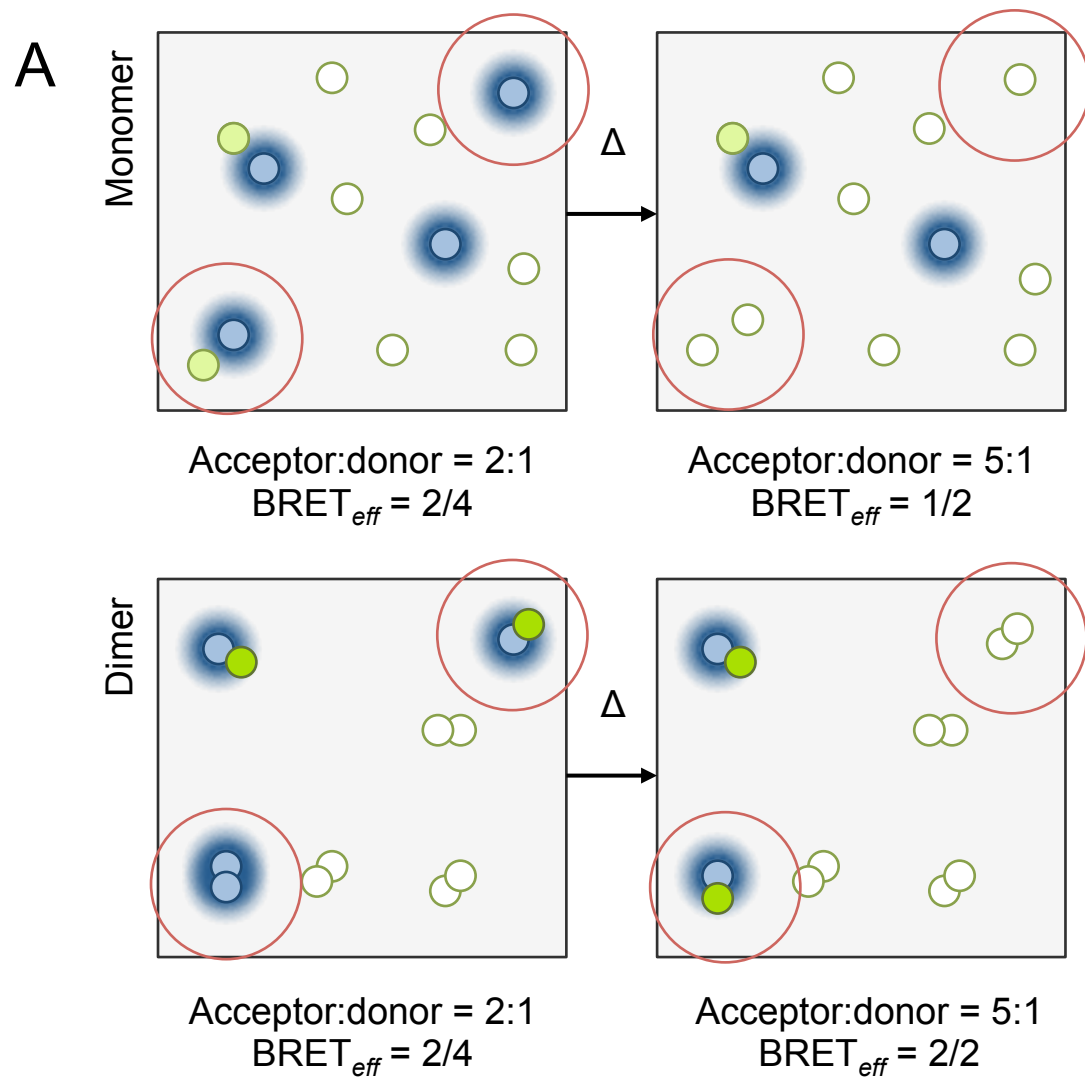


**Table 1** – Published SM imaging studies of *Rhodopsin*-family GPCR stoichiometry.

Study	Receptor(s)	Labeling	Context	Super resolution	Analysis Method	Indirect determination
[43]	$\alpha_2\text{cAR}$ $\beta_1\text{AR}$ LPA1 SIP3	C-terminal SNAP-tag C-terminal HaloTag	Fixed transfected cells	No	TCCD	Controls
[29]	APJ	C-terminal GFP	Live transfected cells	No	Spot intensity analysis	None
[23]	$\beta_1\text{AR}$ $\beta_2\text{AR}$	N-terminal SNAP-tag	Live transfected cells	No	Spot intensity analysis	Controls
[22]	$\beta_2\text{AR}$ mCannR2	C-terminal SNAP-tag C-terminal HaloTag	Fixed transfected cells	No	TCCD	Controls
[27]	D2L D2S D3	N-terminal SNAP-tag Fluorescent antagonist Fluorescent agonist	Live transfected cells	No	Spot intensity analysis	Controls
[8]	FPR	Fluorescent agonist	Live transfected cells	No	Spot intensity analysis	Simulation Controls
[38]	LHR	Fluorescent antibodies	Fixed transfected cells	Yes	Spot association analysis	Simulation
[7]	M1	Fluorescent antagonist	Live transfected cells	No	Spot intensity analysis Photobleach step counting TCCD	Simulation
[28]	M2	Fluorescent antagonist	Live native cells Live transfected cells	No	Photobleach step counting	Simulation
[25]	$\mu\text{-OR}$	N-terminal YFP Direct fluorophore conjugation Fluorescent agonist	High-density lipoprotein particle	No	Photobleach step counting TCCD	None